Dynamic recruitment and activation of ALS-associated TBK1 with its target optineurin are required for efficient mitophagy

Andrew S. Moore[a] and Erika L. F. Holzbaur[a,1]

[a]Department of Physiology, Perelman School of Medicine, University of Pennsylvania, Philadelphia, PA 19104

Edited by Don W. Cleveland, University of California, San Diego, La Jolla, CA, and approved May 2, 2016 (received for review December 2, 2015)

Mitochondria play an essential role in maintaining cellular homeostasis. The removal of damaged or depolarized mitochondria occurs via mitophagy, in which damaged mitochondria are targeted for degradation via ubiquitination induced by PTEN-induced putative kinase 1 (PINK1) and Parkin. Mitophagy receptors, including optineurin (OPTN), nuclear dot 52 kDa protein (NDP52), and Tax1-binding protein 1 (TAX1BP1), are recruited to mitochondria via ubiquitin binding and mediate autophagic engulfment through their association with microtubule-associated protein light chain 3 (LC3). Here, we use live-cell imaging to demonstrate that OPTN, NDP52, and TAX1BP1 are recruited to mitochondria with similar kinetics following either mitochondrial depolarization or localized generation of reactive oxygen species, leading to sequestration by the autophagosome within ∼45 min after insult. Despite this corecruitment, we find that depletion of OPTN, but not NDP52, significantly slows the efficiency of sequestration. OPTN is phosphorylated by the kinase TANK-binding kinase 1 (TBK1) at serine 177; we find that TBK1 is corecruited with OPTN to depolarized mitochondria. Inhibition or depletion of TBK1, or expression of amyotrophic lateral sclerosis (ALS)-associated OPTN or TBK1 mutant blocks efficient autophagosome formation. Together, these results indicate that although there is some functional redundancy among mitophagy receptors, efficient sequestration of damaged mitochondria in response to mitochondrial stress requires both TBK1 and OPTN. Notably, ALS-linked mutations in OPTN and TBK1 can interfere with mitophagy, suggesting that inefficient turnover of damaged mitochondria may represent a key pathophysiological mechanism contributing to neurodegenerative disease.

mitophagy | optineurin | TBK1 | Parkin | amyotrophic lateral sclerosis

Mitochondria form interconnected networks that continuously remodel in response to shifting cellular needs (1). These dynamic networks serve as hubs for diverse cellular functions, including aerobic metabolism, calcium homeostasis (2), and redox signaling (3). Several key mitochondrial functions rely on the potential across the mitochondrial inner membrane. Loss of membrane potential is associated with mitochondrial fragmentation and impaired trafficking (4), and can potentially activate cell death pathways (5). To safeguard against these deleterious outcomes, eukaryotic cells have developed quality control mechanisms to monitor the membrane potential of resident mitochondria and selectively eliminate depolarized organelles through mitophagy.

In mitophagy, damaged mitochondria are recognized and then sequestered by a double-membrane autophagosome, leading to selective degradation. Regulation of this process involves the ubiquitin kinase PTEN-induced putative kinase 1 (PINK1) (6) and the E3-ubiquitin ligase Parkin (7). Specifically, PINK1 accumulates on the surface of depolarized mitochondria, where it phosphorylates ubiquitin on local outer membrane proteins, resulting in the recruitment of Parkin (7–11). Parkin, in turn, modifies additional mitochondrial outer membrane proteins with ubiquitin linkages, which are subsequently phosphorylated by PINK1. The resultant phosphoubiquitin linkages further recruit and activate Parkin, initiating a feed-forward cascade, resulting in the more extensive ubiquitination of mitochondria and the recruitment of the amyotrophic lateral sclerosis (ALS)-associated protein optineurin (OPTN) via its ubiquitin binding in ABIN and NEMO (UBAN) domain (12–14). OPTN induces the formation of a microtubule-associated protein light chain 3 (LC3)-positive autophagosome that engulfs the damaged mitochondrion, effectively sequestering it from the cytosol and ensuring subsequent degradation. The recruitment of Parkin, OPTN, and LC3 to either depolarized or reactive oxygen species (ROS)-damaged mitochondria can occur in as little as 45 min after insult (12), although complete degradation of engulfed mitochondrial fragments requires fusion of autophagosomes with lysosomes and can take up to 24 h (7).

OPTN is a member of a small class of proteins termed autophagy receptors, which, to date, includes at least four other members: p62, nuclear dot 52 kDa protein (NDP52), Tax1-binding protein 1 (TAX1BP1), and next to BRCA1 gene 1 protein (NBR1) (15). Like OPTN, these proteins bind both ubiquitin and LC3 to target ubiquitinated substrates to newly forming autophagosomes. However, the extent to which these other autophagy receptors participate in mitophagy and potentially cooperate with OPTN in the autophagic clearance of depolarized mitochondria is unclear (12–14). Moreover, what role upstream regulators of these proteins, such as TANK-binding kinase 1 (TBK1) (16), may play in this pathway remains unknown. Although NDP52 and TAX1BP1 have recently been shown to be recruited to damaged mitochondria (13, 14), the dynamics of this recruitment have not been investigated. Further, NDP52 has been proposed to function redundantly with OPTN during PINK1/Parkin mitophagy (13, 14), but these studies focused primarily on downstream effects on mitochondrial clearance, rather than the efficiency of mitochondrial sequestration by autophagosomes.

Significance

Mitochondria are key regulators of cellular metabolism and are defective in a number of human disorders. Here, we examine how living cells selectively eliminate damaged mitochondria through the autophagosome-lysosome system. We find that the serine/threonine kinase TANK-binding kinase 1 (TBK1) and its downstream target optineurin (OPTN) are recruited to mitochondria after acute damage, where they coordinate engulfment by autophagosomes. Loss or chemical inhibition of TBK1 stalls mitophagy, resulting in the accumulation of damaged mitochondria. Because mutations in both TBK1 and OPTN are associated with amyotrophic lateral sclerosis and frontotemporal dementia, these results suggest that disordered mitophagy may be associated with selective neurodegeneration.

Author contributions: A.S.M. and E.L.F.H. designed research; A.S.M. performed research; A.S.M. analyzed data; and A.S.M. and E.L.F.H. wrote the paper.

The authors declare no conflict of interest.

This article is a PNAS Direct Submission.

[1]To whom correspondence should be addressed. Email: holzbaur@mail.med.upenn.edu.

This article contains supporting information online at www.pnas.org/lookup/suppl/doi:10.1073/pnas.1523810113/-/DCSupplemental.

Once sequestered within autophagosomes, damaged and potentially toxic mitochondria are functionally separated from the rest of the cell until they can be degraded by lysosomal hydrolases. Thus, the rate at which acutely damaged mitochondria are engulfed by autophagosomes may potently affect cellular homeostasis, with delays leading to toxic cellular insult. Consistent with this possibility, mutations in OPTN cause neurodegeneration, including both ALS and glaucoma, whereas TBK1 mutations also result in ALS and are implicated in frontotemporal dementia (FTD) (17–22).

Here, we use live-cell imaging to examine the dynamics of mitophagy induced by mitochondrial depolarization or localized ROS production. We find that OPTN is required for efficient mitophagy, although other receptors, including NDP52 and TAX1BP1, are recruited to depolarized or damaged mitochondria with similar kinetics. OPTN recruitment occurs coincident with the recruitment of the upstream serine/threonine kinase TBK1. TBK1-dependent phosphorylation of OPTN S177 is not required for OPTN recruitment to Parkin-positive mitochondrial fragments. However, phosphorylation of OPTN at S177 is required for the efficient formation of autophagosomes around depolarized mitochondria. Consistent with this finding, inhibition or depletion of TBK1, or expression of an ALS-associated TBK1 mutant, significantly impairs autophagic engulfment of depolarized mitochondria. Similarly, some, but not all, ALS-linked OPTN mutants disrupt the function of this receptor in mitophagy. Together, these data indicate that efficient sequestration of damaged mitochondria into LC3-positive autophagosomes requires both OPTN and TBK1.

Results

Dynamic Recruitment of Mitophagy Receptors OPTN, NDP52, and TAX1BP1 to Depolarized Mitochondria. We used multicolor live-cell imaging to examine the dynamics of mitophagy following

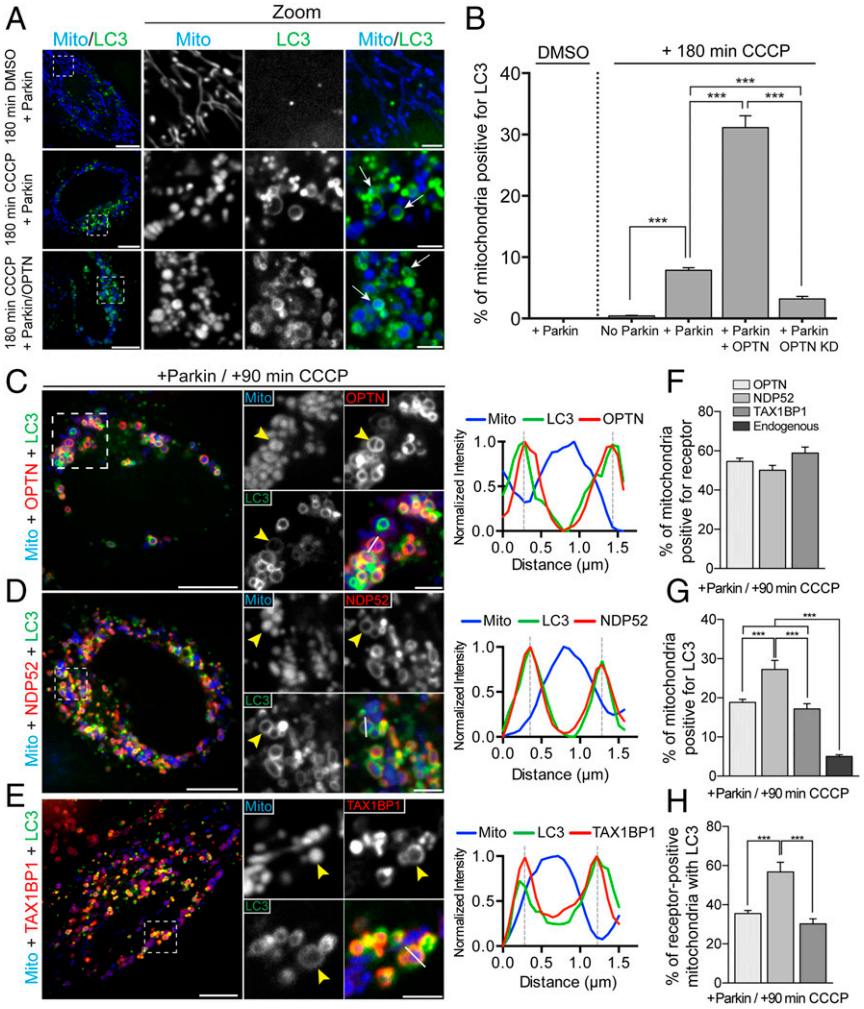

Fig. 1. OPTN, NDP52, and TAX1BP1 are dynamically recruited to depolarized mitochondria after CCCP treatment to initiate autophagosome formation. (*A*) Representative confocal images showing localization of Mito-DsRed2 (blue) and GFP-LC3 (green) in Parkin-expressing HeLa cells treated with either DMSO or 20 μM CCCP. Arrows indicate mitochondria engulfed by autophagosomes. (*B*) Coexpression of OPTN with Parkin enhances mitophagy at 180 min post-CCCP. Depletion of endogenous OPTN significantly reduces mitophagy at this time point. KD, knockdown. (*C–E*) HeLa cells expressing untagged Parkin, Mito-DsRed2, and GFP-LC3, as well as Halo-OPTN (*C*), Halo-NDP52 (*D*), or Halo-TAX1BP1 (*E*) were treated with 20 μM CCCP for 90 min. (*C*) At 90 min post-CCCP, OPTN and LC3 were enriched on the outer surface of fragmented mitochondria (yellow arrowhead). Line scan analysis reveals overlapping OPTN and LC3 local maxima around peak mitochondria (Mito) fluorescence. (*D*) Cells expressing Halo-NDP52 exhibited stable NDP52 and LC3 recruitment to depolarized mitochondria at 90 min post-CCCP (yellow arrowheads). The corresponding line scan indicates NDP52/LC3 colocalization around the indicated mitochondrion. (*E*) Halo-TAX1BP1 also colocalized with LC3 around depolarized mitochondria at 90 min post-CCCP. The line scan shows the corresponding peaks of normalized LC3 and TAX1BP1 intensity. (*F*) OPTN, NDP52, and TAX1BP1 are robustly recruited to mitochondria after 90 min of CCCP treatment. (*G* and *H*) Coexpression of each receptor with Parkin enhances mitophagy at 90 min post-CCCP compared with cells expressing Parkin alone. [Scale bars: *A* and *C–E* (full size), 10 μm; *A* and *C–E* (zoom), 2.5 μm.) Data were collected from 21 to 70 cells from at least three independent experiments. Bars represent mean ± SEM. ***$P < 0.001$.

mitochondrial depolarization in HeLa cells. In control cells, mitochondria form dynamic, interconnected networks with low levels of mitochondrially localized LC3 (Fig. 1*A*, *Top*). To induce mitochondrial depolarization, we treated HeLa cells with 20 μM carbonyl cyanide m-chlorophenylhydrazone (CCCP), a protonophore that triggers rapid loss of mitochondrial membrane potential as indicated by the potentiometric dye tetramethyl rhodamine ethyl ester (TMRE) (Fig. S1 *A*–*C*). Because HeLa cells express low levels of endogenous Parkin (23), CCCP treatment does not induce Parkin-dependent mitophagy in control cells, with less than 1% of mitochondria targeted to autophagosomes at 180 min post-CCCP treatment (Fig. 1*B* and Fig. S1*D*). In contrast, engulfment of depolarized mitochondria can be clearly observed in HeLa cells expressing exogenous Parkin at 180 min post-CCCP, with 8% of mitochondria surrounded by identifiable LC3 rings (Fig. 1 *A* and *B*). As previously shown (12), knockdown of OPTN reduced mitophagy in Parkin-expressing cells, whereas concurrent expression of exogenous OPTN with Parkin resulted in a fourfold increase in LC3-positive mitochondria at this time point (Fig. 1 *A* and *B*), suggesting that cellular expression levels of OPTN may be rate-limiting.

In addition to OPTN, autophagy receptors NDP52 and TAX1BP1 possess the ubiquitin-binding and LC3-interacting region (LIR) motifs required to target ubiquitinated mitochondria to autophagosomes (15). Along with OPTN, NDP52 and TAX1BP1 have been shown to function in the autophagic clearance of invasive bacteria (16, 24, 25), and, more recently, these adaptors have been implicated in the long-term clearance of depolarized mitochondria (13, 14). However, the relative dynamics with which OPTN, NDP52, and TAX1BP1 are recruited to depolarized mitochondria have not been examined. To investigate their recruitment using live-cell assays, we transfected HeLa cells with untagged Parkin, Mito-DsRed2, and GFP-LC3, as well as Halo-OPTN, Halo-NDP52, or Halo-TAX1BP1.

Treating cells with 20 μM CCCP induced the recruitment of OPTN to fragmented mitochondria within 30 min. By 90 min post-CCCP, OPTN was stably enriched on over 50% of mitochondria (Fig. 1 *C* and *F*). NDP52 and TAX1BP1 displayed analogous recruitment kinetics to OPTN, similarly translocating to depolarized mitochondria within 30 min of CCCP treatment. At 90 min post-depolarization, NDP52 localized around 50% of Mito-DsRed2–labeled mitochondrial fragments, whereas TAX1BP1 formed visible rings around 59% of depolarized mitochondria (Fig. 1 *D*–*F*). Although these receptors displayed similar patterns of enrichment on depolarized mitochondria, they differed in their ability to facilitate LC3 recruitment and subsequent mitophagy. Among NDP52-positive mitochondria, 57% were clearly surrounded by GFP-LC3 rings (Fig. 1*H*), indicating efficient sequestration of depolarized mitochondria by the autophagic machinery. In contrast, only 35% of OPTN-positive mitochondria and 30% of TAX1BP1-positive mitochondria were engulfed by autophagosomes at 90 min post-CCCP (Fig. 1*H*). Of note, expression of exogenous OPTN, NDP52, or TAX1BP1 significantly enhanced mitophagy in Parkin-expressing cells compared with cells expressing only endogenous levels of mitophagy receptors (Fig. 1*G*).

In Parkin-expressing HeLa cells transfected with all three autophagy receptors together, we observe robust colocalization of OPTN, NDP52, and TAX1BP1 on mitochondria 90 min post-CCCP (Fig. S2*A*). Recruitment of each of these receptors is dependent on Parkin E3-ligase activity, because expression of the Parkinson's disease-associated Parkin-T240R mutant effectively blocked association of OPTN (12), NDP52, or TAX1BP1 with mitochondria at 1 h post-CCCP (Fig. S2 *B* and *C*). Although direct targeting of an engineered PINK1 construct to mitochondria is sufficient to recruit NDP52 (13), endogenous PINK1 fails to recruit NDP52 to depolarized mitochondria in the absence of exogenous Parkin (Fig. S2*D*).

OPTN, NDP52, and TAX1BP1 Are Recruited to Damaged Mitochondria with Comparable Kinetics. We wondered whether the dynamics of OPTN, NDP52, and TAX1BP1 recruitment differed in response

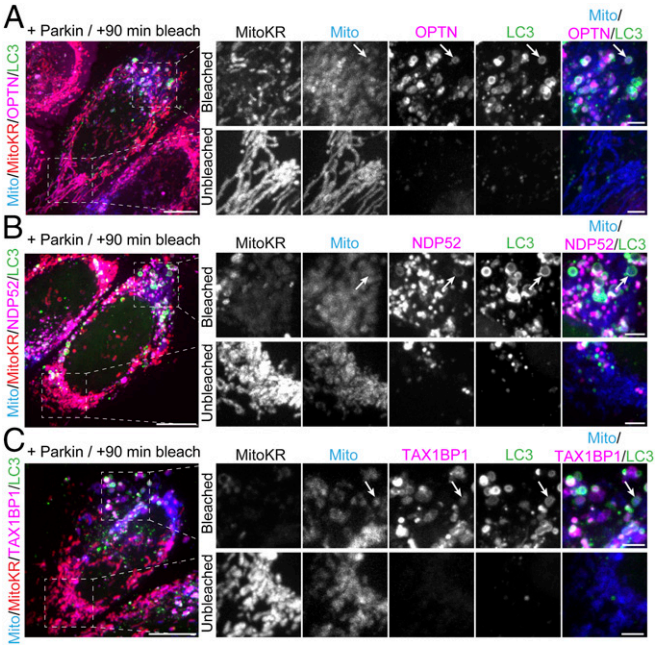

Fig. 2. Focal ROS production induces translocation of LC3 and autophagy receptors to damaged mitochondria. (*Left*) Maximum intensity projections of HeLa cells expressing Parkin, Mito-SNAP (blue), GFP-LC3 (green), and MitoKR (red), as well as Halo-OPTN (*A*), Halo-NDP52 (*B*), or Halo-TAX1BP1 (*C*, magenta) 90 min after activation of MitoKR by 561-nm laser light. (*A*) At 90 min postbleaching, OPTN and LC3 selectively translocate to fragmented mitochondria (arrows) within the bleach window, but not to unbleached mitochondria on the opposite side of the cell. (*B*) At 90 min post-MitoKR activation, NDP52 and LC3 are robustly recruited to bleached mitochondria (arrows). (*C*) TAX1BP1 and LC3 are recruited to damaged mitochondria within the bleach windows 90 min after MitoKR activation (arrows). [Scale bars: *A*–*C* (full size), 10 μm; *A*–*C* (zoom), 2.5 μm.]

to focally induced mitochondrial damage via localized production of ROS. Cells were transfected with untagged Parkin, Mito-SNAP (New England Biolabs), and GFP-LC3, as well as Halo-OPTN, Halo-NDP52, or Halo-TAX1BP1. Cells were also transfected with Mito-KillerRed (MitoKR), a mitochondrially targeted photosensitizer that generates localized production of ROS upon 561-nm laser illumination (26). Before photobleaching, mitochondria double-labeled with MitoKR and Mito-SNAP were highly dynamic and indistinguishable in morphology from mitochondria in cells expressing Mito-DsRed2. We selected one region within each cell and photobleached the MitoKR signal with a 561-nm laser. After bleaching, the MitoKR signal was no longer visible, but mitochondria could still be identified by the photostable Mito-SNAP signal (Fig. S3*A*).

At 90 min after MitoKR photobleaching, we observed robust recruitment of both OPTN and LC3 to bleached mitochondria, but not to mitochondria in unbleached regions of the cell (Fig. 2*A*). In parallel experiments with NDP52 and TAX1BP1, we observed similar recruitment of each receptor to photobleached mitochondria; LC3 was also recruited at this time point (Fig. 2 *B* and *C*).

Next, we investigated the kinetics of OPTN, NDP52, and TAX1BP1 recruitment in response to focal mitochondrial ROS production. Within 15–20 min of MitoKR activation, we observed Parkin recruitment to mitochondria (Fig. S3*B*). Consistent with previous observations (12), OPTN was recruited to bleached mitochondria ~25–30 min after activation of MitoKR (Fig. 3*A* and Movie S1). At this same time point, we observed the initial punctate recruitment of NDP52 to the surface of damaged mitochondria and the formation of weak, but clearly discernible, NDP52 rings around mitochondrial fragments (Fig. 3*B* and Movie S2). In experiments

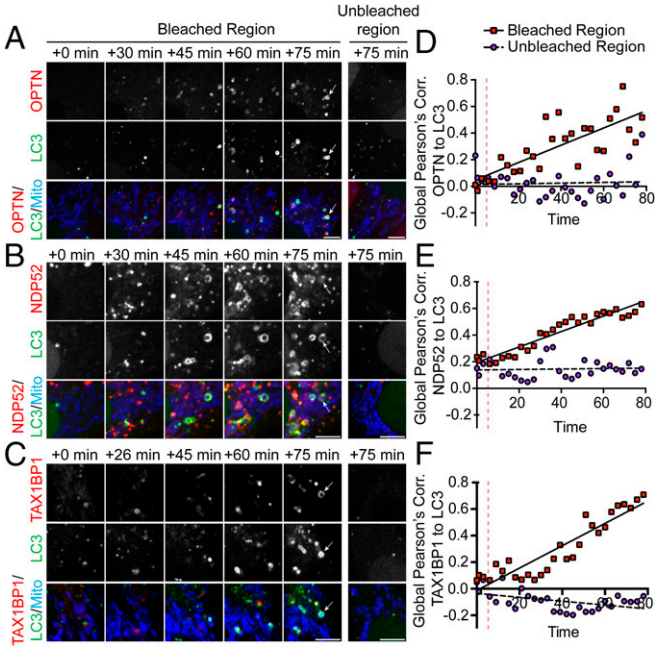

Fig. 3. Autophagy receptor recruitment kinetics. (*A–C*) Confocal time series showing recruitment of autophagy receptors and LC3 to damaged mitochondria after MitoKR activation. OPTN (*A*), NDP52 (*B*), and TAX1BP1 (*C*) begin to accumulate on damaged mitochondria within 30 min. By 45 min, LC3 rings can be visualized forming on receptor-positive mitochondria. At 75 min post-MitoKR, there is significant colocalization of each autophagy receptor with LC3 in the bleached region, but not in distal unbleached regions. (*D–F*) Global Pearson's correlation (Corr.) of each receptor to LC3 increases over time within the bleach window, but not in unbleached regions. (Scale bars: *A–C*, 5 μm.) Vertical dashed lines indicate bleach.

with TAX1BP1, initial recruitment was observed within 20–30 min, with defined TAX1BP1 rings formed around mitochondrial fragments by 30–40 min (Fig. 3*C* and Movie S3). In all experiments, LC3-positive rings could be observed forming around bleached mitochondria within 45 min. (Fig. 3 *A–C*). To determine the rate of autophagosome formation around receptor-positive mitochondria, we calculated the Pearson's correlation coefficient between LC3 and OPTN, NDP52, or TAX1BP1. In all cases, the Pearson's coefficient between LC3 and autophagy receptor significantly increased within the bleach window, but not within a distal unbleached region of equal size (Fig. 3 *D–F*). Together, these results indicate that focal ROS production can initiate OPTN-, NDP52-, and TAX1BP1-dependent mitophagy within a subpopulation of cellular mitochondria.

Although the precise kinetics show some variability from cell to cell or from organelle to organelle, all three receptors tested in live-cell assays were recruited subsequent to Parkin and before LC3. Notably, in our experiments with both MitoKR and CCCP, we observed a two-step recruitment process for OPTN and NDP52. In the 10–15 min immediately following Parkin translocation to damaged mitochondria, low levels of OPTN and NDP52 recruitment were observed, resulting in the formation of uniform, weakly fluorescent rings. When LC3 was subsequently recruited, we observed a robust increase in the autophagy receptor signal intensity (Fig. 4 *A–D*). Although the initial surge in OPTN/NDP52 intensity around mitochondria slightly diminished in the minutes after autophagosome formation, the subpopulation of mitochondria engulfed by LC3 at 90 min displayed significantly higher normalized autophagy receptor fluorescence compared with mitochondria without LC3 (Fig. 4 *E–G*). In contrast, the signal for mCherry-Parkin did not display a similar increase in intensity following mitochondrial engulfment by LC3-positive membranes (Fig. 4*H*).

We used fluorescence recovery after photobleaching (FRAP) to probe the stability of the mitochondrially bound receptors at 90 min post-CCCP, by photobleaching OPTN on mitochondria that either had or had not recruited LC3 (Fig. 4 *I–K*). LC3-negative mitochondria ("−LC3") with dim OPTN rings showed some recovery of fluorescence within 5 min of photobleaching. In contrast, LC3-positive mitochondria ("+LC3") with bright OPTN rings at the time of photobleaching displayed no measurable OPTN recovery over the same time frame (Fig. 4*L*), suggesting that OPTN can cycle on and off of Parkin-positive mitochondria, but becomes stabilized as autophagosomes form.

Depletion of OPTN, but Not NDP52, Blocks Efficient Mitophagy. There have been conflicting reports about the relative contribution of OPTN and NDP52 in mitophagy, and whether these receptors carry out redundant functions (13, 14). To examine this question, we depleted Parkin-expressing cells of either NDP52 or OPTN and investigated levels of mitophagy at 180 min post-CCCP. As previously observed (12), knockdown of endogenous OPTN using siRNA leads to a significant defect in the autophagic engulfment of mitochondria (Fig. 5 *A* and *B*). In contrast, depletion of NDP52 by siRNA (>95% depletion; Fig. S4*A*) had no significant effect on autophagic engulfment of mitochondria at this time point (Fig. 5 *A* and *B*).

A recent study using stable OPTN-knockout HeLa cell lines reported no significant defects in mitochondrial clearance when assayed 1 d after mitochondrial depolarization (13). This observation is seemingly at odds with our observations concerning autophagic engulfment of mitochondria when assayed 180 min after mitochondrial depolarization. To investigate this question, we obtained OPTN and NDP52 knockout cells generated by Lazarou et al. (13) and examined potential differences in mitophagy at time points more closely following mitochondrial depolarization. In the stable OPTN knockout cell line, we noted a modest but significant defect in mitophagy at 180 min post-CCCP (Fig. S4*B*), consistent with our observations in cells with a transient depletion in OPTN (Fig. 5*B*). In contrast, no defect in mitophagy was observed in the NDP52 knockout cell line (Fig. S4*B*), again consistent with our observations in cells in which NDP52 was transiently depleted by siRNA (Fig. 5*B*). Cells with stable knockout of both OPTN and NDP52 showed the most significant defects in mitochondrial engulfment by LC3 at this time point, paralleling the significant defect in mitochondrial clearance at 24 h post-CCCP previously noted in this cell line (13). Thus, OPTN is required for effective mitophagy in the initial hours after mitochondrial damage, although other receptors, such as NDP52, likely compensate over longer time frames, such as 24 h (13).

TBK1 Is Dynamically Corecruited to Depolarized Mitochondria with OPTN. The serine/threonine kinase TBK1 has been implicated in the regulation of multiple receptors, including p62, OPTN, and NDP52 (14, 24, 27). Additionally, immunocytochemistry studies indicate that TBK1 colocalizes with OPTN to intracellular pathogens as well as depolarized mitochondria (16, 27). Based on these observations, we chose to examine the dynamics of TBK1 recruitment in response to mitochondrial depolarization using live-cell imaging. We transfected HeLa cells with SNAP-TBK1, GFP-OPTN, untagged Parkin, and Mito-DsRed2. Before CCCP treatment, both TBK1 and OPTN were distributed throughout the cytoplasm, occasionally localized to small, overlapping foci (Fig. 6*A*, *Top*). Within 10 min of CCCP treatment, these TBK1/OPTN foci disappeared. Over the next 15 min, TBK1 and OPTN translocated onto mitochondria with similar kinetics (Fig. 6 *A* and *B* and Movie S4). Once TBK1 was recruited to depolarized mitochondria, the kinase remained stably associated for over 90 min (Fig. 6*C*). The observed enrichment of TBK1 on depolarized mitochondria was eliminated by depletion of endogenous OPTN (Fig. 6*D*), suggesting that OPTN mediates TBK1 recruitment to mitochondria. Consistent with this hypothesis, overexpression of

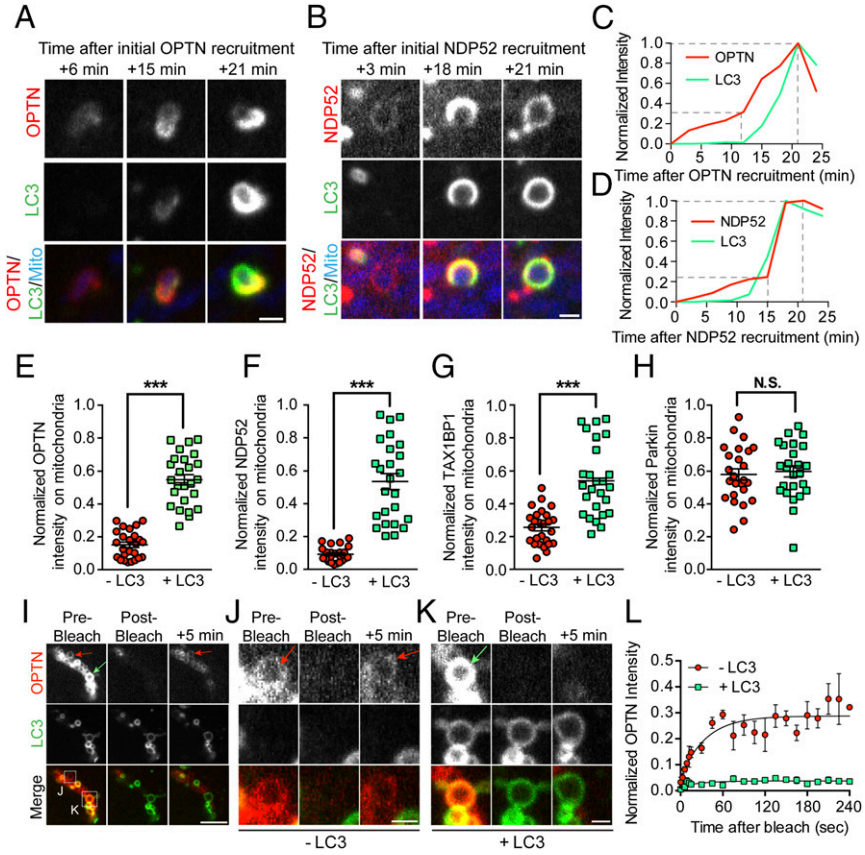

Fig. 4. Autophagy receptors are recruited and stabilized on damaged mitochondria in a two-step process. (*A* and *C*) Before LC3 binding, OPTN is weakly recruited to fragmented mitochondria, gradually increasing in intensity over time. When LC3 is recruited ∼15 min later, OPTN intensity markedly increases before stabilizing with the formed autophagosome at 25 min after initial recruitment. (*B* and *D*) As with OPTN, NDP52 is initially weakly recruited to fragmented mitochondria. NDP52 binding to fragmented mitochondria is enhanced as LC3 rings form and stabilize ∼25 min after initial recruitment. Dashed lines indicate steps of autophagy receptor recruitment. (*E*–*G*) At 90 min post-CCCP, mitochondrially localized autophagy receptors display significantly higher normalized intensity on LC3-positive mitochondria compared with LC3-negative mitochondria. (*H*) At this time point, mitochondrially localized Parkin intensity is not affected by autophagosome formation. (*I*–*K*) To probe the stability of OPTN on mitochondria with or without LC3, OPTN rings on depolarized mitochondria were bleached with 640-nm laser light. (*I*) Confocal time series shows OPTN fluorescence recovery on LC3-negative mitochondria (red arrows) but not LC3-positive mitochondria (green arrow) after photobleaching. (*J*) Magnified view of boxed region in *I* shows clear recovery of OPTN signal intensity 5 min after 640-nm laser bleaching (red arrows). (*K*) Magnified view of boxed region in *I* shows little recovery of OPTN signal 5 min postbleaching (green arrow). (*L*) LC3-negative mitochondria display significantly higher fluorescence recovery after photobleaching. (Scale bars: *I*, 5 μm; *A*, *B*, *J*, and *K*, 1 μm.) In *E*–*H*, $n = 50$ mitochondria from five different cells per comparison. Error bars represent mean ± SEM. In *L*, fluorescence recovery of OPTN is shown in which three mitochondria per condition were fit to a single exponential association model. ***$P < 0.001$. N.S., not significant.

exogenous OPTN enhanced TBK1 association with depolarized, Parkin-positive mitochondria (Fig. 6*E*). Finally, to determine whether TBK1 is corecruited with OPTN, we knocked down endogenous TBK1 and rescued it with either WT-TBK1 or an ALS-associated (TBK1-E696K) mutant that is deficient in OPTN binding (21). At 90 min post-CCCP, WT-TBK1 could be clearly visualized on fragmented mitochondria (Fig. 6*F*, *Top*). In contrast, TBK1-E696K remained cytosolic, failing to associate with depolarized mitochondria (Fig. 6*F*). Thus, we propose that OPTN shuttles TBK1 to depolarized mitochondria.

Activated TBK1 Is Necessary for Efficient Autophagic Engulfment of Depolarized Mitochondria. A recent investigation found that TBK1 is activated through S172 phosphorylation after mitochondrial depolarization (14). However, it is not known whether TBK1 activity is necessary for autophagic engulfment of depolarized mitochondria. To investigate this question, HeLa cells were transfected with untagged Parkin, Mito-DsRed2, GFP-LC3, and either SNAP-TBK1 or Halo-OPTN. Approximately 24 h later, we treated cells for 1 h with either DMSO or 1 μM BX795, a small-molecule inhibitor of TBK1 (28). Before mitochondrial depolarization, cells treated with the TBK1 inhibitor were indistinguishable from those cells that received vehicle control. At 90 min post-CCCP, we observed a clear enrichment of TBK1 on fragmented mitochondria (Fig. S4*A*), indicating that TBK1 recruitment to depolarized mitochondria is not dependent on its phosphorylation state. Consistent with this finding, we also observed robust recruitment of phosphodeficient TBK1-S172A to depolarized mitochondria (Fig. S4*B*). Next, we examined the effect of TBK1 inhibition on OPTN recruitment and autophagosome formation. At 90 min post-CCCP, 66% of mitochondria in cells treated with BX795 were surrounded by OPTN rings (Fig. 7 *B* and *D*), compared with 55% of mitochondria in control cells (Fig. 7 *A* and *D*). Despite this increased recruitment of OPTN, only 4.1% of OPTN-positive mitochondria were engulfed by LC3 in BX795-treated cells (Fig. 7*F* and Fig. S5*C*). In contrast, 35% of OPTN-positive mitochondria in DMSO-treated cells were engulfed by autophagosomes at 90 min post-CCCP (Fig. 7*F*). We observed a similar inhibition of mitophagy in BX795-treated cells depolarized with 10 μM antimycin together with 10 μM oligomycin (Fig. S5*D*).

Depletion of TBK1 by siRNA (>95% depletion; Fig. S5*E*) resulted in a striking decrease in the percentage of LC3-positive mitochondria following 90-min CCCP treatment, comparable to the

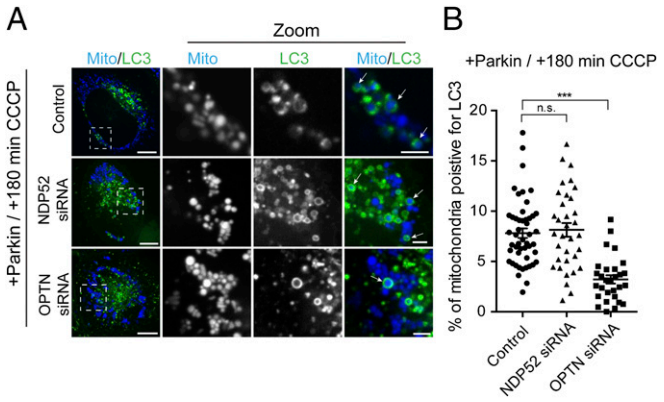

Fig. 5. OPTN depletion blocks efficient mitophagy. (*A*) Representative confocal images of mitochondria-positive autophagosomes at 180 min post-CCCP in Parkin-expressing cells. [Scale bars: *A* (full size), 10 μm; *A* (zoom), 2.5 μm.] (*B*) Depletion of OPTN significantly impairs autophagosome formation at 180 min post-CCCP. In contrast, knockdown of NDP52 does not affect LC3 recruitment to depolarized mitochondria at this time point. Data were collected from 29 to 49 cells from at least three independent experiments. Bars represent mean ± SEM. ***$P < 0.001$. n.s., not significant.

effect observed in cells treated with BX795 (Fig. 6 *C*, *E*, and *F*). This mitophagy defect was rescued by the expression of WT-TBK1, but not by a phosphodeficient TBK1-S172A mutant [WT-TBK1, 20.11 ± 2.1%; TBK1-S172A, 4.9 ± 0.5% (mean ± SEM)]. Of note, knockdown of TBK1 resulted in a slight decrease in OPTN localization to depolarized mitochondria (Fig. 7*D*), suggesting that TBK1 may partially facilitate recruitment and/or retention of OPTN on mitochondria.

TBK1 inhibition or depletion also profoundly impaired the formation of LC3-positive autophagosomes around depolarized mitochondria in cells expressing endogenous levels of autophagy receptor (Fig. 7*G*). In fact, at 180 min post-CCCP, the inhibition of mitophagy observed due to depletion or inhibition of TBK1 was even more extensive than observed upon OPTN knockdown (Fig. 7*G*).

Next, we investigated the effect of TBK1 inhibition on other autophagy receptors. We observed that inhibition of TBK1 by BX795 eliminated the mitophagy enhancement in cells overexpressing OPTN or TAX1BP1, but had only a minor effect on the up-regulated mitophagy observed in cells expressing NDP52 (Fig. 7 *H* and *I*). Both OPTN and NDP52 were still recruited to depolarized mitochondria following TBK1 inhibition, although we did note an ∼50% reduction in TAX1BP1 recruitment (Fig. 7*J*). These observations suggest that OPTN and potentially TAX1BP1 are regulated by TBK1, whereas NDP52 may facilitate mitophagy through a TBK1-independent pathway.

Phosphorylation of OPTN S177 Is Necessary for Efficient Induction of Autophagy Following Mitochondrial Depolarization. OPTN contains a short, four-residue LIR motif near its N terminus (positions 178–181), through which it associates with LC3 (16). The strength of this association, which reflects the ability of OPTN to recruit autophagic membranes, is augmented by TBK1-mediated phosphorylation of a serine residue just before the LIR, at position S177 (16). We thus examined the extent to which phosphorylation of OPTN at S177 influenced the ability of this receptor to mediate autophagosome formation around depolarized mitochondria.

In HeLa cells transfected with Halo-OPTN, Parkin, Mito-DsRed2, and GFP-LC3, 58% of mitochondria were positive for OPTN 90 min after depolarization with CCCP (Fig. 8 *A* and *D*). Autophagosomes effectively formed around these OPTN-positive mitochondria, because 37% were also positive for LC3 (Fig. 8*F*). We then used site-directed mutagenesis to generate a Halo-OPTN construct that could not be phosphorylated at S177 (S177A). Cells were transfected with Halo-OPTN-S177A along with untagged Parkin, Mito-DsRed2, and GFP-LC3. Before CCCP treatment, cells expressing the S177A mutant were indistinguishable from cells expressing WT-OPTN. CCCP treatment induced the translocation of OPTN-S177A to fragmented mitochondria within 20–30 min. At 90 min post-CCCP, OPTN-S177A was uniformly recruited to 75% of the total mitochondrial population (Fig. 8 *B* and *D*). Recruitment of OPTN-S177A to depolarized mitochondria was even more effective than recruitment of WT-OPTN (Fig. 8*D*). Strikingly, however, only 8.1% of OPTN-S177A–positive mitochondria corecruited LC3 (Fig. 8*E*). This dramatic decrease in LC3 recruitment indicates that phosphorylation of OPTN at S177 is necessary for efficient engulfment of depolarized mitochondria by LC3-positive autophagosomes. Interestingly, HeLa cells expressing OPTN-S177A still robustly recruited TBK1 to depolarized mitochondria (Fig. S6*A*), indicating that recruitment of TBK1 to depolarized mitochondria is not dependent on OPTN S177 phosphorylation.

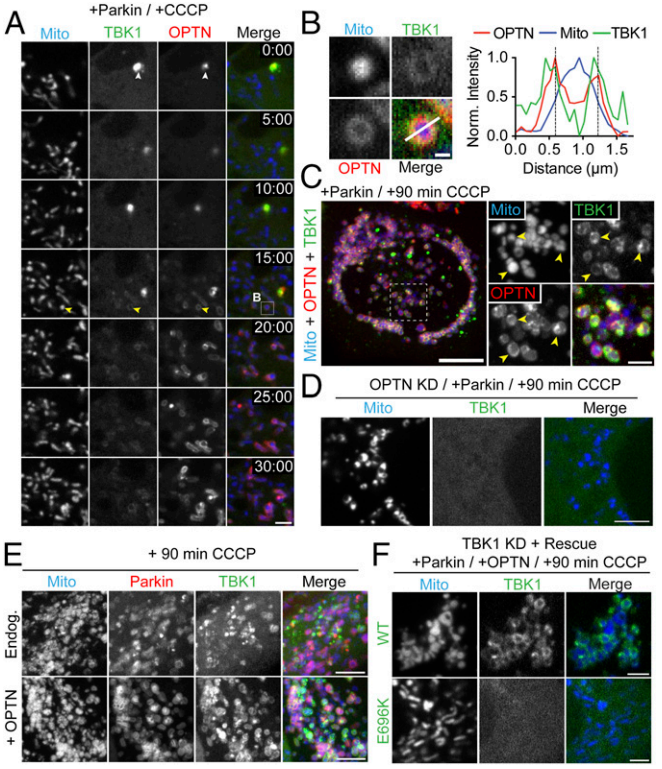

Fig. 6. TBK1 is corecruited with OPTN to depolarized mitochondria. (*A*) Time series tracking recruitment of SNAP-TBK1 (green) and GFP-OPTN (red) to depolarized mitochondria in a Parkin-expressing cell. The time stamp indicates elapsed time since addition of CCCP (minutes:seconds). Immediately after CCCP treatment, OPTN and TBK1 are largely cytosolic but colocalize in small puncta (white arrowheads). At 15 min post-CCCP, both OPTN and TBK1 begin to appear on fragmented mitochondria (yellow arrowheads). (*B*) Magnified view of boxed region in *A* with corresponding line scan indicating TBK1/OPTN colocalization on an individual mitochondrion. Norm., normalized. (*C*) Confocal z-stack showing recruitment of OPTN and TBK1 to fragmented mitochondria (yellow arrowheads) 90 min post-CCCP treatment. (*D*) Depletion of OPTN eliminates TBK1 recruitment to depolarized mitochondria. (*E*) Overexpression of OPTN enhances TBK1 recruitment to Parkin-positive mitochondria at 90 min post-CCCP. Endog., endogenous. (*F*) Endogenous TBK1 was depleted and rescued with either WT-TBK1 (*Top*) or an ALS-linked TBK1 mutant unable to bind OPTN (E696K, *Bottom*). WT-TBK1 was clearly enriched on fragmented mitochondria after CCCP treatment, whereas TBK1-E696K remained cytosolic. [Scale bars: *C* (full size), 10 μm; *A*, *D*, and *E*, 5 μm; *F* and *C* (zoom), 2.5 μm; *B*, 0.5 μm.]

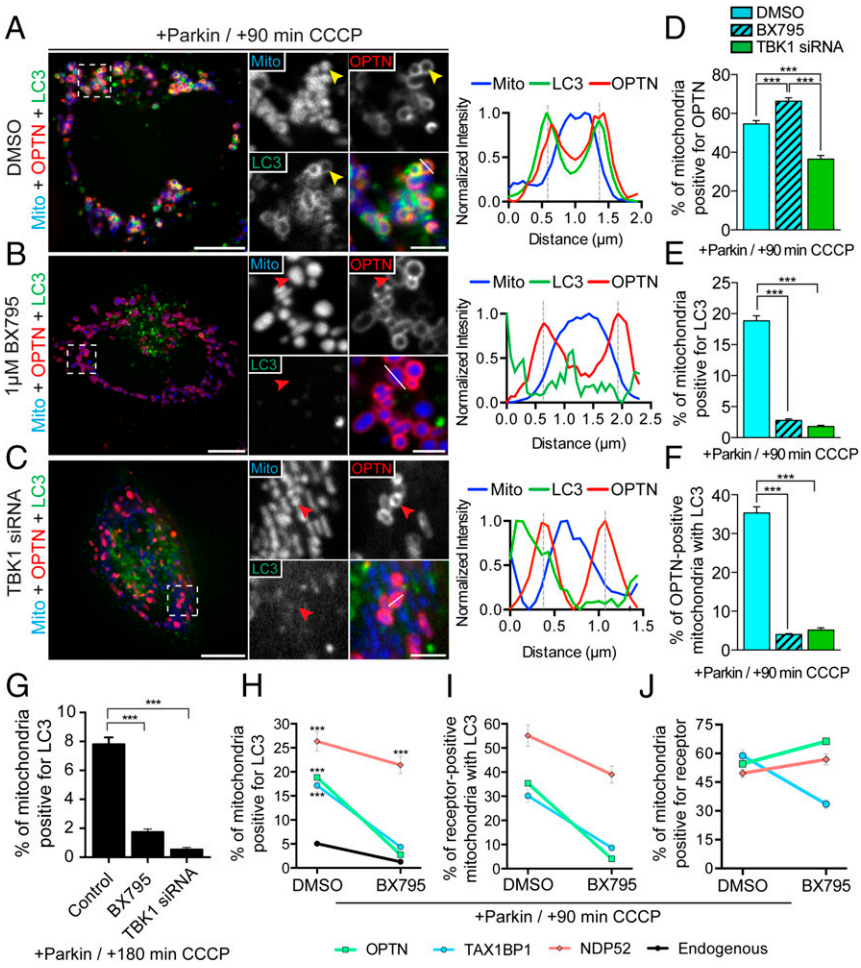

Fig. 7. TBK1 is required for efficient autophagic engulfment of depolarized mitochondria. (*A–C*) HeLa cells expressing untagged Parkin, Mito-DsRed2 (blue), Halo-OPTN (red), and GFP-LC3 (green). (*A*) Representative confocal image of DMSO-pretreated HeLa cell at 90 min post-CCCP with the corresponding line scan. OPTN and LC3 stably localize on the surface of damaged mitochondria (yellow arrowheads). (*B*) Pretreatment with 1 μM BX795 significantly attenuates LC3, but not OPTN, recruitment to depolarized mitochondria (red arrowheads). The corresponding line scan indicates increased OPTN, but not LC3, fluorescence around the peak mitochondrial intensity. (*C*) TBK1 depletion blocks association of LC3 with fragmented mitochondria at 90 min post-CCCP (red arrowheads). The line scan indicates OPTN, but not LC3, recruitment to fragmented mitochondria. (*D*) Inhibition of TBK1 by BX795 increases the proportion of cellular mitochondria that recruit OPTN, whereas knockdown of TBK1 decreases OPTN-positive mitochondria. (*E* and *F*) Both TBK1 knockdown and inhibition by BX795 significantly impair autophagosome formation on OPTN-positive mitochondria at 90 min post-CCCP. (*G*) In Parkin-expressing cells, depletion or inhibition of TBK1 interferes with mitophagy at 180 min post-CCCP. (*H*) Coexpression of Parkin with either OPTN or TAX1BP1 significantly enhances mitophagy at 90 min post-CCCP in control cells, but not in cells treated with a TBK1 inhibitor. In contrast, coexpression of Parkin with NDP52 robustly enhances mitophagy independent of TBK1 activity. (*I*) NDP52-positive mitochondria, but not OPTN- or TAX1BP1-positive mitochondria, are efficiently engulfed by autophagosomes after TBK1 inhibition. (*J*) TAX1BP1 recruitment to depolarized mitochondria is diminished in cells pretreated with BX795. [Scale bars: *A–C* (full size), 10 μm; *A–C* (zoom), 2.5 μm.] Data were collected from 19 to 61 cells from at least three independent experiments. Bars represent mean ± SEM. ***$P < 0.001$.

We next asked whether expression of a constitutively active, phosphomimetic form of OPTN would enhance CCCP-induced mitophagy. Cells expressing the phosphomimetic construct Halo-OPTN-S177E as well as Parkin, Mito-DsRed2, and GFP-LC3 appeared phenotypically normal before addition of CCCP. Addition of CCCP induced robust recruitment of OPTN-S177E to depolarized mitochondria (Fig. 8 *C* and *D*) and clear formation of LC3-positive autophagosomes around the OPTN-positive mitochondria (Fig. 8*F*). However, we did not see an up-regulation of either OPTN or LC3 recruitment to mitochondria in comparison to cells expressing WT-OPTN (Fig. 8 *D–F*), suggesting that OPTN is efficiently phosphorylated in CCCP-treated HeLa cells. Together, these results indicate that activation of OPTN through S177 phosphorylation is essential for its ability to function as an autophagy receptor for depolarized mitochondria.

ALS-Associated OPTN and TBK1 Mutants Interfere with Mitophagy of Depolarized Mitochondria. In the past several years, multiple mutations in both OPTN and TBK1 have been identified in patients with ALS and FTD (17–22). We therefore examined whether these disease-associated mutations interfere with efficient mitophagy. We depleted endogenous TBK1 with an siRNA specific for the 3′ UTR of TBK1 (leading to a 75% reduction in endogenous levels of TBK1; Fig. S7 *A* and *B*) and transfected cells with Halo-OPTN, Parkin, Mito-DsRed2, and GFP-LC3. Depletion of TBK1 resulted in a significant decrease in LC3-positive mitochondria at 90 min post-CCCP compared with cells transfected with a scrambled siRNA (Fig. 9*A*). This mitophagy defect was rescued by expression of WT-TBK1, but not by an ALS-associated TBK1-E696K mutant (Fig. 9 *A* and *B*). TBK1-E696K did not associate with OPTN, and failed to translocate to depolarized mitochondria 90 min after CCCP treatment (Fig. 9*B*).

Next, we asked whether ALS-associated OPTN mutations similarly interfered with recruitment of LC3 to depolarized mitochondria. We examined three ALS-associated OPTN mutants: (*i*) OPTN-E478G (ubiquitin-binding domain mutant), (*ii*) OPTN-R96L (coiled-coil domain 1 mutant), and (*iii*) OPTN-Q398X (truncation mutant entirely lacking UBAN domain). As previously shown, expression of WT-OPTN in Parkin-expressing cells results in a robust enhancement of mitophagy at 90 min post-CCCP. To examine whether these ALS-associated OPTN mutants could similarly enhance mitophagy, we transfected cells with untagged Parkin, mCh-LC3, and Mito-SNAP, as well as GFP-OPTN, GFP-OPTN-E478G, GFP-OPTN-Q398X, or GFP-OPTN-R96L. Both OPTN-E478G and OPTN-Q398X remained cytosolic at 90 min post-CCCP, failing to translocate to depolarized mitochondria and enhance mitophagy (Fig. 9 *C* and *D*). In contrast, both WT-OPTN and OPTN-R96L translocated to depolarized, fragmented mitochondria, inducing equivalent levels of autophagosome formation (Fig. 9 *C* and *D*). Thus, expression of some, but not all, ALS-linked mutations in OPTN can disrupt efficient mitophagy.

Discussion

In this study, we used live-cell imaging to examine the dynamics of autophagy receptors and their regulation during selective mitophagy. Previously, we found that the ALS-associated receptor OPTN mediates the autophagic engulfment of Parkin-positive mitochondria (12). Here, we examined the regulation of OPTN by TBK1, an upstream kinase also linked to ALS. We find that TBK1

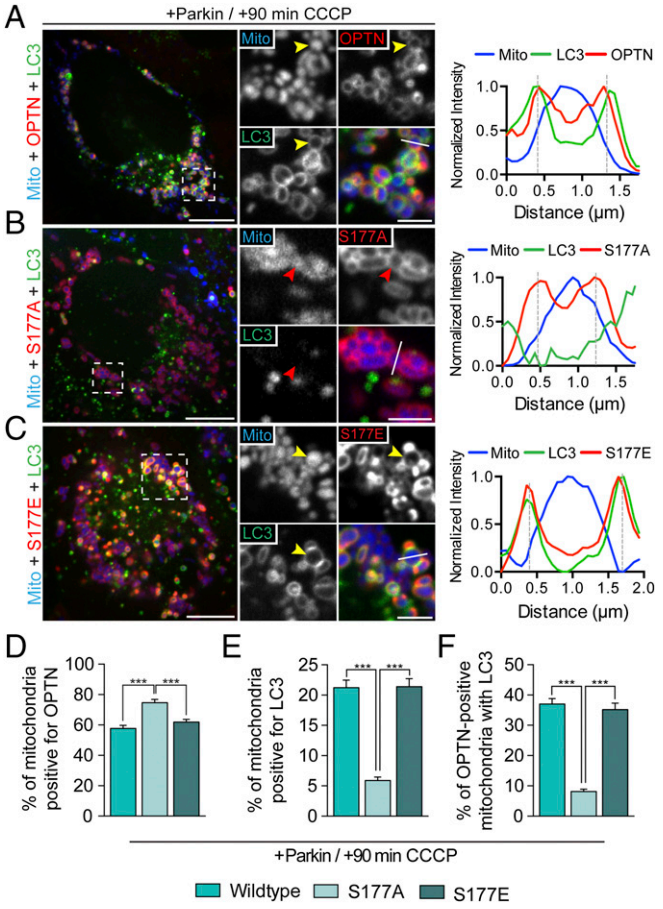

Fig. 8. OPTN S177 phosphorylation is required for efficient mitophagy. HeLa cells expressing untagged Parkin, Mito-DsRed2, and GFP-LC3, as well as WT-OPTN (*A*), OPTN-S177A (*B*), or OPTN-S177E (*C*) were treated with 20 μM CCCP for 90 min. (*A*) At 90 min post-CCCP, WT-OPTN and LC3 are enriched on the outer surface of mitochondria (yellow arrowheads). Line scan analysis through the indicated mitochondrion shows overlapping OPTN and LC3 local maxima. (*B*) Cells expressing OPTN-S177A show clear recruitment of phosphodeficient OPTN to fragmented mitochondria, but fail to recruit LC3 efficiently after CCCP treatment (red arrowheads). The corresponding line scan indicates S177A, but not LC3, localization to mitochondria. (*C*) Phosphomimetic OPTN-S177E, like WT, translocates with LC3 to the surface of mitochondria after CCCP treatment (yellow arrowheads). A line scan shows S177E/LC3 colocalization around mitochondria. (*D–F*) Phosphodeficient OPTN is robustly recruited to mitochondria after CCCP treatment compared with WT-OPTN or S177E, but blocks recruitment of LC3. [Scale bars: *A–C* (full size), 10 μm; *A–C* (zoom), 2.5 μm.] Data were collected from 25 to 41 cells from at least three independent experiments. Bars represent mean ± SEM. ***$P < 0.001$.

is dynamically recruited with OPTN to depolarized, Parkin-positive mitochondria. Inhibition of TBK1 does not hinder the initial recruitment of OPTN, but does dramatically inhibit the assembly of autophagic membranes around depolarized mitochondria. Because knockdown of TBK1 resulted in a more significant inhibition of LC3 recruitment than we observed following OPTN knockdown, our observations support a model in which multiple receptors contribute to the mitophagy of damaged mitochondria. Specifically, we found that two other autophagy receptors, NDP52 and TAX1BP1, are recruited with similar kinetics to depolarized, Parkin-positive mitochondria. Overexpression of any of these three receptors enhances the formation of autophagosomes around depolarized mitochondria, suggesting that cellular expression levels of these receptors may be limiting. However, we noted that NDP52 depletion had little effect on the kinetics of sequestration of depolarized mitochondria over a time frame of up to 3 h, in contrast to our observations on OPTN depletion. Thus, although there may be functional compensation over longer time frames (13), kinetically, these receptors are not interchangeable.

A recent investigation reported that stable knockout of OPTN in HeLa cells did not have a significant effect on mitochondrial clearance 24 h after depolarization (13). Using the same knockout line, we observed a modest but significant 20% decrease in the formation of mitochondrial autophagosomes at 3 h post-CCCP. Thus, loss of OPTN affects the efficiency of autophagosome formation in both knockdown and knockout paradigms. However, at longer time points, both OPTN knockdown and knockout HeLa cells can effectively clear damaged mitochondria, likely through recruitment of alternative receptors, such as NDP52. This question has been addressed in detail in bacterial autophagy, or xenophagy, where the interplay among autophagy receptors is essential for efficient autophagosomal engulfment of invasive pathogens (29). Here, we show that multiple receptors are recruited to depolarized mitochondria with similar kinetics, yet these receptors are only partially redundant in effecting efficient mitochondrial engulfment.

Studies on xenophagy have also identified a key regulatory role for TBK1, a serine/threonine kinase that has been demonstrated to interact with OPTN, NDP52, and TAX1BP1 (16, 24, 25). Here, we found that OPTN and TBK1 translocate to depolarized mitochondria with similar kinetics. OPTN likely shuttles TBK1 to damaged mitochondria, because depletion of OPTN or expression of a TBK1 mutant unable to bind OPTN eliminates recruitment of TBK1 to depolarized mitochondria. However, recruitment of OPTN is not dependent on TBK1 expression or TBK1

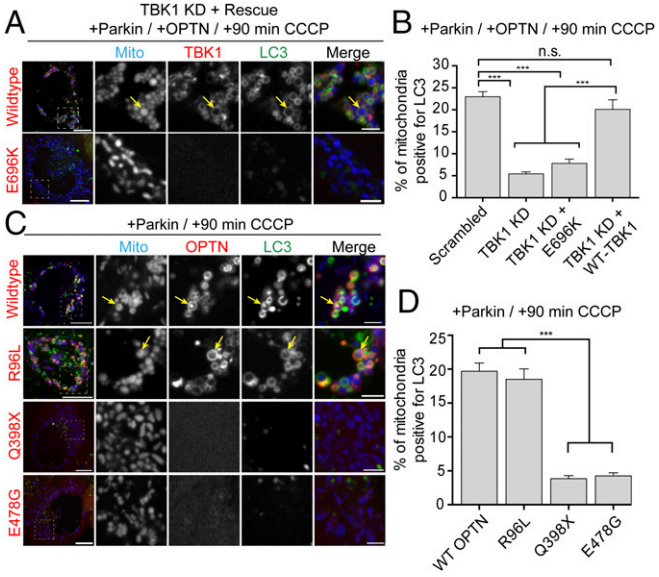

Fig. 9. ALS-associated TBK1 and OPTN mutants block mitophagy. (*A*) Representative confocal images of Parkin/OPTN-expressing HeLa cells in which endogenous TBK1 has been knocked down and rescued with either WT-TBK1 or TBK1-E696K. (*B*) TBK1 depletion significantly blocks mitophagy at 90 min post-CCCP compared with scrambled control. Expression of WT-TBK1, but not ALS-linked TBK1-E696K, rescues this mitophagy defect. (*C*) Representative confocal images of HeLa cells expressing untagged Parkin, mCherry-LC3 (green), and Mito-SNAP (blue), as well as GFP-OPTN, GFP-OPTN-R96L, GFP-OPTN-E478G, or GFP-OPTN-Q398X (red) at 90 min post-CCCP. Although WT-OPTN and OPTN-R96L colocalize with LC3 on fragmented mitochondria after CCCP treatment (yellow arrows), both OPTN-Q398X and OPTN-E478G remain cytosolic. (*D*) At 90 min post-CCCP, OPTN-R96L and WT-OPTN enhance mitophagy, whereas cells expressing OPTN-Q398X and OPTN-E478G show significantly lower levels of LC3-positive mitochondria. [Scale bars: *A* and *B* (full size), 10 μm; *A* and *B* (zoom), 2.5 μm.] Data were collected from 21 to 33 cells from at least thee independent experiments. Bars represent mean ± SEM. ***$P < 0.001$.

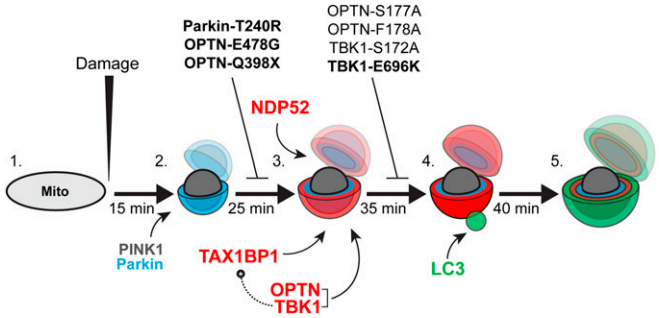

Fig. 10. Model depicting autophagy receptor recruitment to depolarized mitochondria over time. (1) Before a depolarizing injury, mitochondria are elongated and motile. (2) Within 15 min of injury, damaged mitochondria recruit PINK1 and Parkin, resulting in the phosphoubiquitination of outer membrane proteins and mitochondrial fragmentation. (3) Twenty-five minutes after initial damage, and within ~10 min of the first Parkin recruitment, autophagy receptors OPTN, TAX1BP1, and NDP52 are weakly recruited to the surface of fragmented mitochondria. OPTN shuttles its upstream kinase TBK1 to the mitochondrial surface. Expression of the Parkinson's disease-associated Parkin-T240R mutant blocks recruitment of all three receptors. Additionally, ALS-linked OPTN-E478G and OPTN-Q398X mutants are not recruited to ubiquitinated mitochondria. (4) Within 5–10 min of weak autophagy receptor recruitment, a small number of mitochondria display enhanced autophagy receptor recruitment and stabilization, coincident with the recruitment of the autophagosome membrane protein LC3. This step is dependent on TBK1 phosphorylation of OPTN S177, and is blocked in cells expressing ALS-linked TBK1-E696K. Although OPTN and TAX1BP1 depend on TBK1 activity in this pathway, NDP52 can stabilize on mitochondria and facilitate autophagic engulfment of mitochondria even in the absence of TBK1. Thus, high levels of NDP52 can compensate for OPTN or TBK1 loss of function. (5) By 40–45 min after the initial damage, fully formed autophagosomes develop around mitochondria, effectively sequestering the damaged organelles from the surrounding cytosol. Bolded mutants have been linked to neurodegenerative disease.

activity; similarly, TAX1BP1 and NDP52 are also recruited to depolarized mitochondria when TBK1 is inhibited.

Although inhibition of TBK1 does not interfere with the initial recruitment of OPTN to mitochondria, it does block the stabilization of OPTN and the concomitant recruitment of LC3 to depolarized mitochondria, suggesting that mitochondrially localized OPTN must be subsequently activated by TBK1 to function as an autophagy receptor. In contrast, NDP52 can facilitate the formation of autophagosomes on depolarized mitochondria, even in the absence of TBK1. This finding suggests that OPTN and TAX1BP1 act in the same pathway downstream of TBK1, whereas NDP52 may function in a parallel mitophagy pathway less dependent on TBK1 (Fig. 10), as initially suggested by Lazarou et al. (13).

In these studies, we induced mitophagy using several approaches, including depolarization by the mitochondrial uncoupler CCCP, inhibition of the electron transport chain by antimycin and oligomycin, and ROS production by activation of a localized photosensitizer (MitoKR). Irrespective of the upstream damage, we observed very similar recruitment kinetics for the autophagy receptors and consistent timing of LC3 recruitment to form autophagosomes around depolarized mitochondria. Typically, OPTN, NDP52, and TAX1BP1 display a weak pattern of recruitment to depolarized mitochondria 10–15 min after recruitment of Parkin. Starting 10 min after this weak recruitment, a small subset of mitochondria displays enhanced receptor intensity coupled to more stable receptor binding, coincident with the recruitment of LC3 puncta. Over the next ~5 min, LC3 puncta develop into spherical structures entirely circumscribing depolarized, Parkin-positive mitochondria.

By 90 min after CCCP-induced depolarization, nearly every mitochondrion is Parkin-positive; more than half show clear autophagy receptor rings, but only 25% are effectively sequestered by LC3-positive autophagosomes. Even at longer time points, such as 5 h or 8 h post-CCCP, a number of OPTN-positive mitochondria can still be clearly seen outside of autophagosomes. The variability in efficiency with which individual mitochondria are targeted to autophagosomes after cell-wide depolarization may be limited by several factors, including expression levels of autophagy receptors; the relative activation of upstream regulatory signals, such as TBK1; and possibly the availability of autophagic membrane sources, and thus the rate of autophagosome biogenesis. However, the sooner depolarized mitochondria are quarantined from the rest of the cell by autophagosomes, the less damage they are likely to cause. Therefore, the rate at which damaged mitochondria are effectively engulfed and sequestered by an isolation membrane may be among the most important aspects of mitophagy.

A recent exome sequencing study identified significantly higher rates of TBK1 polymorphisms in individuals with ALS (30). Another study linked loss-of-function TBK1 mutations to both ALS and FTD (21). Finally, mutations in both TBK1 and OPTN are causal for both ALS and glaucoma (20, 31). In this study, we observed that the ALS-associated mutants TBK1-E696K, OPTN-E478G, and OPTN-Q398X all interfere with efficient autophagic engulfment of damaged mitochondria. However, we did not observe mitophagy defects in cells expressing OPTN-R96L. Thus, disordered mitophagy may contribute to the pathophysiology of ALS and FTD, but further work is required to establish this point fully. Specifically, slower and/or less effective mitophagy might lead to the accumulation of damaged mitochondria and subsequent cytotoxic stress. Consistent with the late-onset nature of both ALS and glaucoma, other receptors likely compensate to some degree, but the decreased efficiency caused by TBK1 or OPTN mutations may be sufficient to lead to enhanced neurodegeneration over time.

It is not yet clear why mutations in ubiquitously expressed proteins result in selective degeneration of specific neuronal populations. Perhaps expression levels of compensatory mitophagy receptors, such as NDP52, are limiting in affected cells. Consistent with this hypothesis, levels of NDP52 protein are comparatively low in human brain lysates (13). Alternatively, the effects of dysregulated mitochondrial quality control might simply manifest in specific neuronal populations earlier and to a greater extent than other cell types. Motor neurons and retinal ganglion cells affected in ALS and glaucoma are characterized by extended axonal processes; whether damaged mitochondria occupying distal axonal regions are subject to the same quality control mechanisms as those mechanisms near the cell body remains unclear (32, 33). It is also a distinct possibility that mutations in TBK1 and OPTN contribute to disease through other mechanisms, including aberrant protein aggregate autophagy (aggrephagy) or neuroinflammatory pathways; further work will be required to address these possibilities.

Methods

Constructs, siRNAs, and Antibodies. Constructs used include the following: Mito-DsRed2 (a gift from T. Schwarz, Harvard Medical School, Boston) recloned into SNAP-Tag (New England Biolabs) and psBFP2-C1 (Addgene); TBK1 (no. 23851; Addgene) recloned into pSNAPf vector; pEGFP-LC3 (a gift from T. Yoshimori, Osaka University, Osaka) recloned with pmCherry (Takara Bio, Inc.); YFP-Parkin and mCherry-Parkin (gifts from R. Youle, NIH, Bethesda); untagged Parkin, pEGFP-OPTN, and pEGFP-OPTN-E478G (gifts from I. Dikic, Goethe University, Frankfurt) recloned with pmCherry and HaloTag (Promega); R96L-EGFP (no. 68846; Addgene); Q398X-EGFP (no. 68849; Addgene); HaloTag-NDP52 (Promega) recloned into pEGFP; HaloTag-TAX1BP1 (Promega) recloned into pEGFP (Promega); and pKillerRed-dMito (Evrogen). Site-directed mutagenesis was used to generate mCherry-Parkin-T240R, HaloTag-OPTN-S177A, HaloTag-OPTN-S177E, SNAP-TBK1-S172A, and SNAP-TBK1-E696K. HaloTag constructs were labeled with either HaloTag tetramethyl rhodamine ligand (G821; Promega) or silicon-rhodamine-Halo ligand (a gift from L. Reymond and K. Johnsson, Ecole

Polytechnique Federale de Lausanne, Lausanne, Switzerland). SNAP-Tag constructs were labeled with SNAP-Cell 647-SiR (S9102S; New England Biolabs) or SNAP-Cell 430 (S9109S; New England Biolabs). The siRNA oligos used include the following: OPTN siRNA 1 (ON-TARGET*Plus SMARTpool*; Dharmacon), OPTN siRNA 2 (5′-CCACCAGCTGAAAGAAGCC-3′; Dharmacon), TBK1 siRNA (h) (sc-39058; Santa Cruz Biotechnology), TBK1 3′ UTR siRNA (Dharmacon), SignalSilence NDP52 siRNA I (8964S; Cell Signaling), and fluorescent ON-TARGET*Plus* Non-targeting siRNA no. 1 with 5′ Cy5 (Dharmacon). Antibodies used include the following: OPTN (ab23666; Abcam), TBK1/NAK (ab40676; Abcam), NDP52 (ab68588; Abcam), GAPDH (ab9494; Abcam), and actin (MAB1501; Calbiochem).

Cell Culture, Reagents, and Live Imaging. HeLa cells were maintained in DMEM (Corning) with 10% (vol/vol) FBS and 1% Glutamax, and kept at 37 °C in a 5% CO_2 incubator. Twenty-four hours before transfection, cells were plated on uncoated, 35-mm, glass-bottom dishes (P35G-0-20-C; MatTek). DNA constructs were transfected 18–24 h before imaging using FuGene 6 (E2691; Promega). The siRNAs were transfected 48 h before imaging with Lipofectamine RNAiMAx (13778030; Thermo Fisher). Transfection efficiency for both DNA and RNA was typically >90%. To assess mitochondrial membrane potential, cells were loaded with 30 nM TMRE (T-669; Life Technologies) for 30 min, followed by two washes in complete media. SNAP and HaloTag ligands were applied at 2.5 μM. SNAP-tag ligand was applied for 30 min, followed by two washes and a 30-min washout. Halo-tag was applied for 15 min, followed by two washes in complete media. OPTN, NDP52, and OPTN/NDP52 knockout HeLa cell lines (gifts from R. Youle, NIH, Bethesda) were maintained in identical conditions as WT HeLa cell lines. Before imaging, HeLa cell culture media were replaced with imaging media [DMEM without phenol red + 25 mM Hepes (Corning), with 10% (vol/vol) FBS and 1% Glutamax]. Cells were then transferred to a Nikon Eclipse Ti Microscope housed within a 37 °C environment chamber and imaged at a magnification of 100× (apochromat, 1.49-N.A. oil immersion objective) using an UltraView Vox spinning disk confocal imaging system (PerkinElmer). Mitochondrial depolarization was induced by bath application of 20 μM cyanide m-chlorophenyl hydrazone (C2759; Sigma–Aldrich) or 10 μM Antimycin A (A8674; Sigma–Aldrich) with 10 μM oligomycin (pool of A, B, and C; 04876; Sigma–Aldrich). Mitophagy in cells expressing both Parkin and autophagy receptors was assessed at 90 min post-CCCP, whereas cells expressing Parkin alone were analyzed at 180 min post-CCCP. For TBK1 inhibition experiments, cells were pretreated with 1 μM BX795 (204001; Calbiochem) for 1 h before CCCP treatment. Still-frame images, z-stacks, and time-lapse movies were acquired using Volocity image acquisition software (PerkinElmer). Focal mitochondrial damage was induced through photoirradiation of MitoKR by 561-nm laser light. Specifically, two ∼15 × 15-μm regions were bleached with a 561-nm laser for 100 cycles lasting no longer than 3 min in total. For FRAP experiments, HaloTag-OPTN rings at 90 min post-CCCP were bleached with a 640-nm laser at 100% for 100 cycles at a rate of 1 ms per cycle. Standard immunoblot analysis of whole-cell lysates confirmed NDP52 and TBK1 knockdown (Fig. S4 *E* and *G*).

Image Analysis and Statistics. Mito-DsRed2 fragments, GFP-LC3 rings, HaloTag-OPTN rings, HaloTag-NDP52 rings, and HaloTag-TAX1BP1 rings were manually counted in ImageJ (NIH) and Volocity. Only clearly defined mitochondrially localized rings were counted. Two-pixel-wide line scans through mitochondria were generated in ImageJ, normalized in Excel (Microsoft), and graphed in Prism (GraphPad). Autophagy receptor and LC3 ring intensity was calculated as the average intensity of the two highest peak values along line scans and normalized per cell and condition. TMRE and Mito-SNAP fluorescence intensity was calculated as the mean intensity along two-pixel-wide line scans. Global Pearson's correlations for bleached and unbleached regions were generated in Volocity. Z-projections and time-lapse movies were generated in ImageJ, and 3D renderings were produced in Volocity. Statistical analyses were carried out on datasets consisting of at least three independent experiments, using a two-tailed, unpaired Student's *t* test comparing two groups; one-way ANOVA with Tukey's multiple comparison test when comparing more than two groups; or two-way ANOVA with Tukey's multiple comparison test when comparing the main effects of autophagy receptor (OPTN, NDP52, TAX1BP1, or endogenous) and treatment (DMSO or BX795). Error bars indicate mean ± SEM. Images and figures were prepared in Illustrator (Adobe).

ACKNOWLEDGMENTS. We thank Yvette Wong for advice and discussion, and Mariko Tokito for assistance in construct design and cloning. We acknowledge funding from NIH Grant R37 NS060698 (to E.L.F.H.).

1. McBride HM, Neuspiel M, Wasiak S (2006) Mitochondria: More than just a powerhouse. *Curr Biol* 16(14):R551–R560.
2. Pizzo P, Drago I, Filadi R, Pozzan T (2012) Mitochondrial Ca^{2+} homeostasis: Mechanism, role, and tissue specificities. *Pflugers Arch* 464(1):3–17.
3. Chandel NS (2014) Mitochondria as signaling organelles. *BMC Biol* 12:34.
4. Wang X, et al. (2011) PINK1 and Parkin target Miro for phosphorylation and degradation to arrest mitochondrial motility. *Cell* 147(4):893–906.
5. Summers DW, DiAntonio A, Milbrandt J (2014) Mitochondrial dysfunction induces Sarm1-dependent cell death in sensory neurons. *J Neurosci* 34(28):9338–9350.
6. Zheng X, Hunter T (2014) Pink1, the first ubiquitin kinase. *EMBO J* 33(15):1621–1623.
7. Narendra D, Tanaka A, Suen D-FF, Youle RJ (2008) Parkin is recruited selectively to impaired mitochondria and promotes their autophagy. *J Cell Biol* 183(5):795–803.
8. Matsuda N, et al. (2010) PINK1 stabilized by mitochondrial depolarization recruits Parkin to damaged mitochondria and activates latent Parkin for mitophagy. *J Cell Biol* 189(2):211–221.
9. Narendra DP, et al. (2010) PINK1 is selectively stabilized on impaired mitochondria to activate Parkin. *PLoS Biol* 8(1):e1000298.
10. Kane LA, et al. (2014) PINK1 phosphorylates ubiquitin to activate Parkin E3 ubiquitin ligase activity. *J Cell Biol* 205(2):143–153.
11. Koyano F, et al. (2014) Ubiquitin is phosphorylated by PINK1 to activate parkin. *Nature* 510(7503):162–166.
12. Wong YC, Holzbaur EL (2014) Optineurin is an autophagy receptor for damaged mitochondria in parkin-mediated mitophagy that is disrupted by an ALS-linked mutation. *Proc Natl Acad Sci USA* 111(42):E4439–E4448.
13. Lazarou M, et al. (2015) The ubiquitin kinase PINK1 recruits autophagy receptors to induce mitophagy. *Nature* 524(7565):309–314.
14. Heo J-MM, Ordureau A, Paulo JA, Rinehart J, Harper JW (2015) The PINK1-PARKIN Mitochondrial Ubiquitylation Pathway Drives a Program of OPTN/NDP52 Recruitment and TBK1 Activation to Promote Mitophagy. *Mol Cell* 60(1):7–20.
15. Rogov V, Dötsch V, Johansen T, Kirkin V (2014) Interactions between autophagy receptors and ubiquitin-like proteins form the molecular basis for selective autophagy. *Mol Cell* 53(2):167–178.
16. Wild P, et al. (2011) Phosphorylation of the autophagy receptor optineurin restricts Salmonella growth. *Science* 333(6039):228–233.
17. Maruyama H, Kawakami H (2013) Optineurin and amyotrophic lateral sclerosis. *Geriatr Gerontol Int* 13(3):528–532.
18. Ito H, et al. (2011) Clinicopathologic study on an ALS family with a heterozygous E478G optineurin mutation. *Acta Neuropathol* 122(2):223–229.
19. Weishaupt JH, et al. (2013) A novel optineurin truncating mutation and three glaucoma-associated missense variants in patients with familial amyotrophic lateral sclerosis in Germany. *Neurobiol Aging* 34(5):1516.e9–1516.e15.
20. Pottier C, et al. (2015) Whole-genome sequencing reveals important role for TBK1 and OPTN mutations in frontotemporal lobar degeneration without motor neuron disease. *Acta Neuropathol* 130(1):77–92.
21. Freischmidt A, et al. (2015) Haploinsufficiency of TBK1 causes familial ALS and frontotemporal dementia. *Nat Neurosci* 18(5):631–636.
22. Cady J, et al. (2015) Amyotrophic lateral sclerosis onset is influenced by the burden of rare variants in known amyotrophic lateral sclerosis genes. *Ann Neurol* 77(1):100–113.
23. Pawlyk AC, et al. (2003) Novel monoclonal antibodies demonstrate biochemical variation of brain parkin with age. *J Biol Chem* 278(48):48120–48128.
24. Thurston TL, Ryzhakov G, Bloor S, von Muhlinen N, Randow F (2009) The TBK1 adaptor and autophagy receptor NDP52 restricts the proliferation of ubiquitin-coated bacteria. *Nat Immunol* 10(11):1215–1221.
25. Tumbarello DA, et al. (2015) The Autophagy Receptor TAX1BP1 and the Molecular Motor Myosin VI Are Required for Clearance of Salmonella Typhimurium by Autophagy. *PLoS Pathog* 11(10):e1005174.
26. Yang J-Y, Yang WY (2011) Spatiotemporally controlled initiation of Parkin-mediated mitophagy within single cells. *Autophagy* 7(10):1230–1238.
27. Matsumoto G, Shimogori T, Hattori N, Nukina N (2015) TBK1 controls autophagosomal engulfment of polyubiquitinated mitochondria through p62/SQSTM1 phosphorylation. *Hum Mol Genet* 24(15):4429–4442.
28. Clark K, et al. (2011) Novel cross-talk within the IKK family controls innate immunity. *Biochem J* 434(1):93–104.
29. Boyle KB, Randow F (2013) The role of 'eat-me' signals and autophagy cargo receptors in innate immunity. *Curr Opin Microbiol* 16(3):339–348.
30. Cirulli ET, et al.; FALS Sequencing Consortium (2015) Exome sequencing in amyotrophic lateral sclerosis identifies risk genes and pathways. *Science* 347(6229):1436–1441.
31. Sirohi K, Kumari A, Radha V, Swarup G (2015) A Glaucoma-Associated Variant of Optineurin, M98K, Activates Tbk1 to Enhance Autophagosome Formation and Retinal Cell Death Dependent on Ser177 Phosphorylation of Optineurin. *PLoS One* 10(9):e0138289.
32. Cai Q, Zakaria HM, Simone A, Sheng Z-H (2012) Spatial parkin translocation and degradation of damaged mitochondria via mitophagy in live cortical neurons. *Curr Biol* 22(6):545–552.
33. Ashrafi G, Schlehe JS, LaVoie MJ, Schwarz TL (2014) Mitophagy of damaged mitochondria occurs locally in distal neuronal axons and requires PINK1 and Parkin. *J Cell Biol* 206(5):655–670.